

# A Fast Shutdown Technique for Large Tokamaks

S. C. Jardin, G. L. Schmidt, E. Fredrickson, K. Hill,  
J. Hyun<sup>1</sup>, B. J. Merrill<sup>2</sup>, R. Sayer<sup>3</sup>,

*Princeton Plasma Physics Laboratory  
P.O. Box 451, Princeton, NJ 08543*

*September 16, 1999*

## Abstract

A practical method is proposed for the fast shutdown of a large ignited tokamak. The method consists of injecting a rapid series of 30-50 deuterium pellets doped with a small ( 0.0005%) concentration of Krypton impurity, and simultaneously ramping the plasma current and shaping fields down over a period of several seconds using the poloidal field system. Detailed modeling with the Tokamak Simulation Code using a newly developed pellet mass deposition model shows that this method should terminate the discharge in a controlled and stable way without producing significant numbers of runaway electrons. A partial prototyping of this technique was accomplished in TFTR.

## 1 Introduction

One of the major impediments facing acceptance of a large-scale power-producing tokamak is the threat of an unmitigated full-current plasma disruption. The possibility of a sudden loss of over a Giga-Joule of thermal energy and the resulting rapid quench of tens of Mega-Amperes of plasma current places severe design restrictions on the construction of a next step device and could significantly affect it's operation and availability schedule. These considerations motivate the development of disruption avoidance and mitigation techniques that are applicable to power-producing scale tokamaks. One of these techniques that needs to be developed and demonstrated is a method for shutting the tokamak down and reducing it's current to zero in a time that is much shorter than the natural current decay time. This would allow emergency termination of a discharge in the event it was concluded that a system failure was about to occur and/or that a major disruption was inevitable.

---

<sup>1</sup>Fusion Energy Research Program, University of Maryland, College Park, MD

<sup>2</sup>Idaho National Engineering and Environmental Laboratory, Idaho Falls, ID

<sup>3</sup>Computational Physics and Engineering Division, Oak Ridge National Laboratory, Oak Ridge, TN

Kuteev, et. al. [1] proposed a relatively benign technique for emergency termination of such a discharge involving the injection of a pellet of a high-Z noble gas such as Krypton. Subsequent analysis [2] supported by zero and one-dimensional [3] simulations of this process revealed that the situation is greatly complicated by the prospect that large numbers of runaway electrons could be generated, in effect converting the discharge into a long-lived runaway discharge. While there has been some experimental interest in the impurity injection technique in present day tokamaks [4] [5], it has been concluded by several authors that for future high temperature, high current tokamaks, the injection of massive amounts of low-Z material such as deuterium [3] [7] would best minimize runaway electron production, and that this might be feasible by using a multiple pellet train or perhaps a liquid jet [8]. However, this technique is yet to be demonstrated either by detailed simulation or by experimental testing.

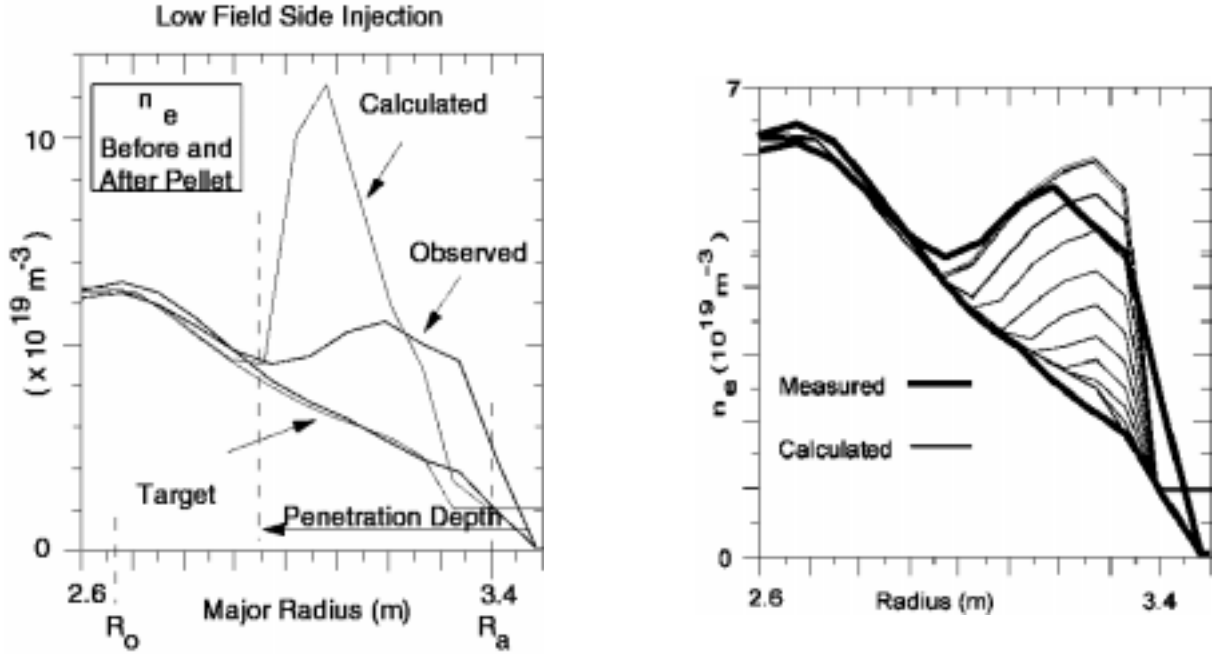
In this paper, we propose a variation on the impurity injection plasma termination technique. Our method differs from those described earlier by two distinguishing features: (1) it requires the injection of a train of 30-50 pellets of low-Z material, (ie, deuterium) doped with a trace of high-Z impurity (ie, Krypton) and (2) it requires a simultaneous controlled ramp-down of the the poloidal field coils. The small concentration of Krypton causes the plasma to radiate away the stored thermal and magnetic energy in a time of a few seconds, while the ramping down of the PF coils prevents the development of the vertical displacement event while aiding the controlled current rampdown. We use a realistic 2D plasma simulation to demonstrate that this method is effective in producing a controlled plasma shutdown without generating significant runaways, and that it should work over a large operational window in parameter space.

## 2 Physics Models

The physics model used in this analysis is contained in the Tokamak Simulation Code (TSC) [9] [10] [11] which has been modified to include models of impurity doped pellet injection, of runaway current generation, and a more realistic model of radiative loss due to impurities. The tokamak plasma is assumed to be 2D (axisymmetric), throughout and to pass through a sequence of equilibrium states. As described in Ref. [9], the plasma equilibrium is “free boundary” in the sense that it is compatible with the instantaneous currents in the poloidal field coil system and the induced currents in the structure, which are themselves computed from self-consistent circuit equations. The plasma energy and particle densities are computed from the standard set of flux-surface averaged (1-1/2D) evolution equations [10] with the pellet fueling and radiation appearing as source and sink terms, respectively.

### 2.1 Pellet Model

The pellet injection density source model is that of an ablating pellet injected from the outer (low toroidal field side) plasma midplane with an initial velocity aimed towards the plasma magnetic axis. The spherical pellet, assumed to be deuterium doped with a small fraction  $f_I$  of high-Z noble gas impurity, with instantaneous radius  $r_p$ (cm) passing through background plasma with electron temperature  $T_e$ (eV) and electron density



a. Density data from TFTR shot 75934 in which a 1100 m/s D pellet of radius 1.75 mm was injected and calculation (final time) without backaveraging

b. Density data from TFTR and calculation (intermediate times shown) with 80% backaveraging applied

Figure 1:

$n_e(cm^{-3})$  ablates mass at the rate (atoms/sec) given by [1]

$$\frac{dN}{dt} = \alpha T_e^{\frac{5}{3}} n_e^{\frac{1}{3}} r_p^{\frac{4}{3}} \quad (1)$$

where  $\alpha = 8.89 \times 10^{15}$ . While this pellet ablation model is in good agreement with experiment [12] regarding depth of pellet penetration, it is not in general agreement regarding local plasma mass increase if that increase is interpreted in the normal way that the ablated pellet mass is deposited locally at the instantaneous position of the pellet. An illustration of this apparent disagreement of the simple model and experiment is shown in Fig. 1a where the results of straightforward implementation of Eq. 1 interpreted as a mass source in a TSC simulation of pellet injection experiments in TFTR is shown.

To account for this discrepancy in local mass for those experiments using pellets injected from the large major radius side as we propose here, we have developed an empirical “backaveraged” model [13] of pellet mass distribution in which the ablated material is uniformly added to the plasma on the flux surfaces exterior to that where the instantaneous ablation is occurring. Thus if  $\hat{\psi}$  is the normalized plasma poloidal magnetic flux that is zero at the magnetic axis and unity at the plasma vacuum boundary, and if  $V(\hat{\psi})$  is the

plasma volume contained within the surface  $\hat{\psi}$ , then for the 100% backaveraged model, as the pellet is passing over flux surface  $\hat{\psi}'$ , the atoms ablated from the pellet according to Eq. 1 are deposited uniformly (per unit volume) over the plasma volume exterior to the surface  $\hat{\psi}'$  plus some scrape-off layer volume. The new plasma mass added to the scrape-off layer is immediately lost, but this region is needed to account for the less than 100% efficiency observed in outside launch pellet experiments.

As discussed in [13], and illustrated in Fig. 1b, detailed comparison with TFTR data shows that a better fit with experimental density measurements immediately after the pellet injection is obtained by using a 20/80/20 split variation of this model such that 20% of the pellet mass is deposited where it is ablated and the remaining 80% is backaveraged as described here, with the scrape-off layer volume taken to be 20% of the plasma volume. For the other calculations described in this paper, a 20/80/00 split was used which is identical to that used in the TFTR modeling except that no scrape-off layer volume was included in the backaveraging because of the increased pellet velocities and penetration distances. While this model is largely empirical, it is motivated by the recent 3D MHD simulations of Strauss et. al. [17] which show that the sudden localized pressure perturbation induced by the pellet cause a rapid transport of mass towards the low-field-side of the torus.

## 2.2 Runaway Electron Model

The runaway production modeling in TSC treats both the Dreicer and the Fleischman-Rosenbluth avalanche [14] production mechanisms. The Dreicer production rate equation used in TSC,  $S_D$ , is that proposed by Cohen [15]. The Rosenbluth model [16] for avalanche runaway electron formation has also been incorporated into the TSC code, and is always the dominant mechanism for the calculations presented here. In the TSC implementation, the parallel electric field comes from the modified Ohm's law, projected in the direction parallel to the magnetic field,

$$E_{\parallel} = \eta_{\parallel}(j_{\parallel} - j_{RA}) \quad (2)$$

where  $\eta_{\parallel}$  is the parallel resistivity,  $j_{\parallel} = \frac{\vec{B}}{B} \cdot \nabla \times \vec{B}$  is the (total) current density parallel to the magnetic field, and  $j_{RA}$  is the runaway current density obtained from the formula

$$\frac{\partial j_{RA}}{\partial t} = \frac{j_{RA}}{\tau \ln \Lambda} \sqrt{\frac{\pi \gamma}{3(Z+5)}} \left( \frac{E_{\parallel}}{E_C} - 1 \right) \left( 1 - \frac{E_C}{E_{\parallel}} + \frac{4\pi(Z+1)^2}{3\gamma(Z+5) \left( \frac{E_{\parallel}^2}{E_C^2} + \frac{4}{\gamma^2} - 1 \right)} \right)^{-\frac{1}{2}} + S_D + S_{RA} \quad (3)$$

Here,

$$E_c = \frac{2\pi e^3(n_e + n_T)}{mc^2} \ln \Lambda \quad (4)$$

is the ‘‘critical’’ electric field strength with  $n_T$  being the total electron density including free and bound electrons,

$$\gamma = (1 + 1.46\sqrt{r/R} + 1.72r/R)^{-1} \quad \text{and} \quad \tau = \frac{mc}{eE_c}$$

where  $\tau$  represents runaway collision time(s). The initial source of runaways is taken to be

$$S_{RA} = 8.6 \times 10^{-23} n_T (m^{-3}) \frac{amps}{m^2}$$

### 2.3 Particle Transport and Radiation Model

TSC solves the the impurity ion transport equations that self-consistently accounts for the impurity charge state and emitted radiation. The following impurity evolution equation is solved for each impurity charge state [18], [19]:

$$\frac{\partial N^q}{\partial t} + \frac{\partial}{\partial \Phi}(N^q \Gamma \cdot \nabla \Phi) = I^{q-1} N^{q-1} - (I^q + R^q) N^q + R^{q+1} N^{q+1} + S_N^q \quad (5)$$

where  $N^q \equiv n^q \frac{\partial V}{\partial \Phi}$  is the flux-surface averaged differential number density for charge state  $q$ ,  $\Phi$  is the normalized plasma toroidal magnetic flux that is zero at the magnetic axis and one at the plasma/vacuum boundary,  $I^q$  and  $R^q$  are ionization and recombination rate coefficients, and  $S_N^q$  is the mass source term which is zero for  $q > 0$ , and defined as in section 2.1 for  $q = 0$ . For the deuterium density, the ionization and recombination terms are absent, and in addition to the pellet density source described in section 2.1, an additional edge density source is included of the form

$$S = 6.0 \times 10^{20} \exp^{3(\Phi-1)} \text{m}^{-3} \text{s}^{-1}.$$

The particle flux  $\Gamma$  is given by

$$n^q \Gamma \cdot \nabla \Phi = -D |\nabla \Phi|^2 \left( \frac{\partial n^q}{\partial \Phi} + \frac{n^q}{\Phi} \right) \quad (6)$$

where  $D$  is a diffusion coefficient taken to be

$$D = \begin{cases} 0.15 + 3.0 \Phi^2 \frac{\text{m}^2}{\text{sec}} & \text{for } \Phi < 0.75 \\ 0.5 \frac{\text{m}^2}{\text{sec}} & \text{for } \Phi > 0.75 \end{cases}$$

This form was found to give good agreement for simulations of TFTR data[13].

The radiant power release from electron collisional excitation of and radiative recombination with these impurities is obtained by summing the radiant contribution from all impurity charge states, including neutrals, as follows,

$$P_{ir} = \sum_q n^q n_e \mathcal{L}^q \quad (7)$$

where  $\mathcal{L}$  is the radiant rate coefficient and  $n_e$  is the plasma electron density. The rate coefficients for this transport model are obtained by interpolation of data tables generated with the ‘‘average ion’’ atomic physics model described in Ref. [20]

## 3 Modeling Result

The fast shutdown technique being proposed here has the following elements: (1) At the shutdown initiation time  $t = t_i$ , begin injection of a sequence of  $N$  deuterium pellets of radius  $r_P$  doped with  $X\%$  Krypton impurity, with a velocity of  $V_P$  and a spacing of  $t_\delta$  between pellets, and (2) Simultaneous with this, starting at time  $t = t_i$ , ramp the preprogrammed currents in each of the tokamak poloidal field coils (PF coils) to zero in

a time  $t_{Ramp}$ , but keeping the vertical control and radial control feedback systems turned on.

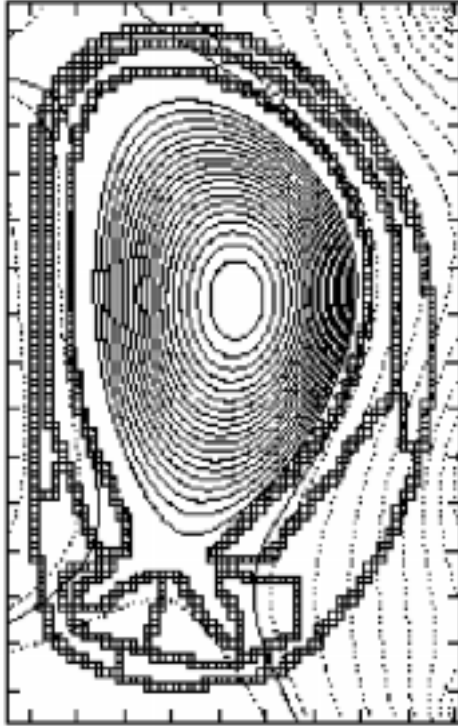
Each of the  $N$  pellets in the sequence will penetrate slightly further towards the plasma magnetic axis than the pellet before it due to the preceding pellets lowering the background plasma temperature through a combination of densification and radiation. At the end of the pellet sequence, the Krypton impurity will be distributed fairly uniformly throughout the plasma, causing the plasma pressure and temperature profiles to remain relatively invariant as the Krypton radiates away most of the initial stored energy and the subsequent energy generated through ohmic heating.

The ramp-down of the PF coil currents accomplishes two things. First, it reverses the loop voltage at the outermost edge of the plasma, effectively removing the outer flux surfaces and the current associated with them. This reduces the plasma current, including the runaway current, and also counters the tendency for new runaway electrons to form near the edge. Second, the ramp-down of the PF coil currents reduces the plasma shaping fields, causing the formerly elongated plasma to take on a more circular shape, and to thus become stable with respect to vertical displacements. This can be thought of as a natural reversal of the process by which the current channel was layered in and the plasma was originally shaped. The plasma can thus be made to remain on or near the tokamak midplane as it's toroidal current decreases to zero in a time  $t \sim t_{Ramp}$ .

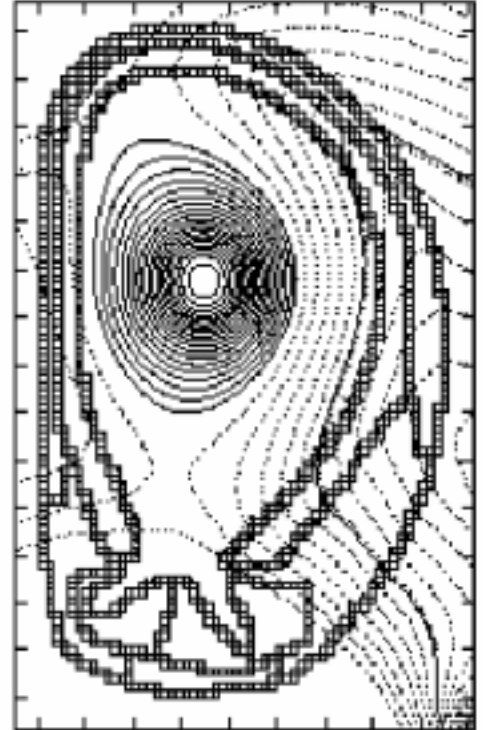
Another consideration is that the plasma remain stable to MHD instabilities throughout this sequence. Since the pressure is decreasing in an almost self-similar way (ie., keeping it's same normalized spatial profile shape), the pressure driven instabilities should not be unstable, and the remaining modes of concern are kink and tearing modes associated with the plasma current and the current profile. We thus monitor the trajectory of the plasma discharge in the  $(l_i, q_{Edge})$  space in [21] to verify that it remains in the stable region during the rapid current ramp-down. This is made possible by the fact that the radiation cools the plasma and greatly reduces the current diffusion time, allowing the PF coils to ramp the current down over this much shortened time.

In this section we illustrate the application of this technique to provide a benign rapid shutdown sequence for an early design of the proposed International Thermonuclear Experimental Reactor, ITER [22]. In this simulation, which we will refer to as the “standard sequence”, a train of  $N = 35$  pellets is injected on the plasma midplane with inward radial velocity of  $V_P = 3700\text{m/s}$  and separation between pellets of  $t_\delta = 5$  ms. Each pellet is a radius  $r_P = 6$  mm sphere of deuterium doped with  $X = 0.0005\%$  Krypton. Simultaneous with the start of the pellet injection, all the tokamak PF coil currents are ramped down to zero linearly over a time  $t_{Ramp} = 4.0$  s although the feedback systems controlling vertical and radial positions are left on. The poloidal magnetic flux surfaces at the beginning and the end of this sequence,  $t = t_i$  and  $t = t_i + 2.4$  s, are illustrated in Fig. 2. A summary of the total plasma current vs time is given in Fig. 3. No significant runaway electron current was generated in this sequence, and it remained MHD stable throughout.

We now examine some of the features of this simulation in more detail. In Fig. 4ab we plot a close-up of the individual pellet penetration distances and the associated radiative power during the first 200 ms of the sequence. We see that there is an accompanying increase of radiation as the Krypton in each pellet ionizes, and that this energy loss due to both line and bremsstrahlung radiation plus the increased deuterium density brought by the pellet causes the local background temperature to lower enough so the subsequent



a. Poloidal Flux at initial stage, time  $t = t_i$ , plasma current  $I_P = 24MA$ .



b. Poloidal Flux at final stage, time  $t = t_i + 2.4 s$ , plasma current  $I_P \approx 3MA$ .

Figure 2:

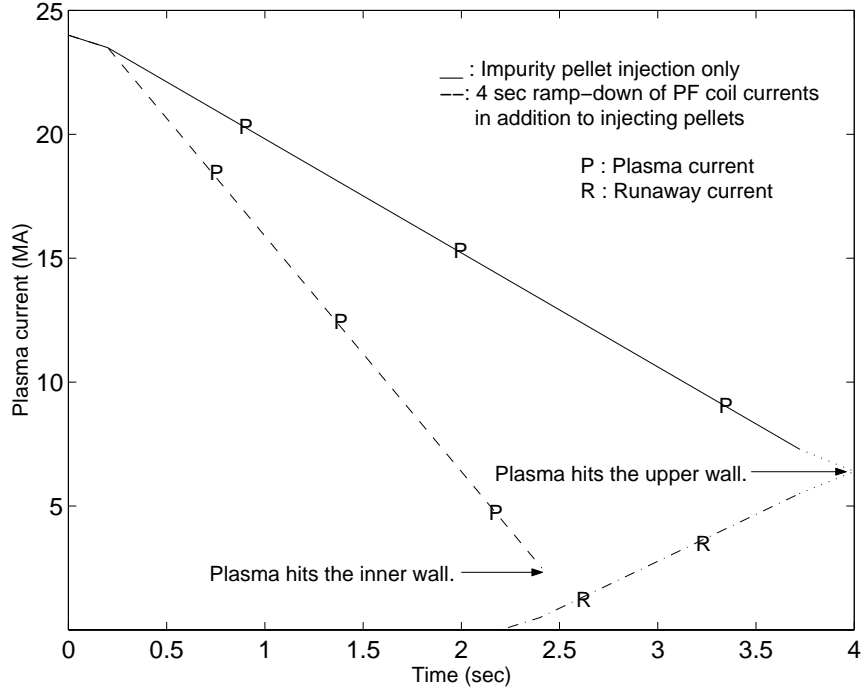


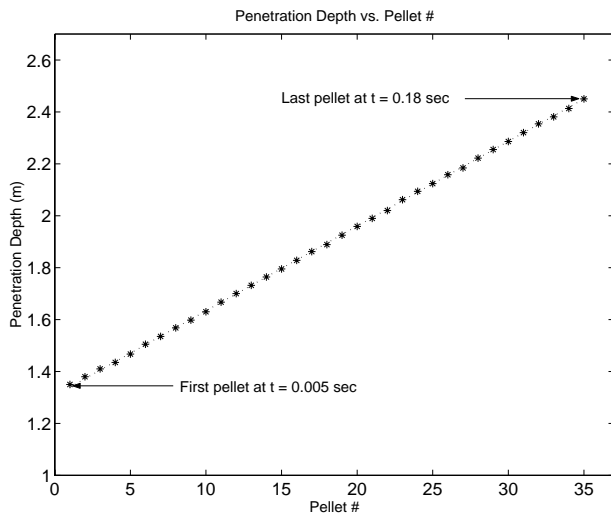
Figure 3: The current quench as a function of time

pellets can penetrate incrementally further, with the final pellet penetrating through 2.4 m of plasma.

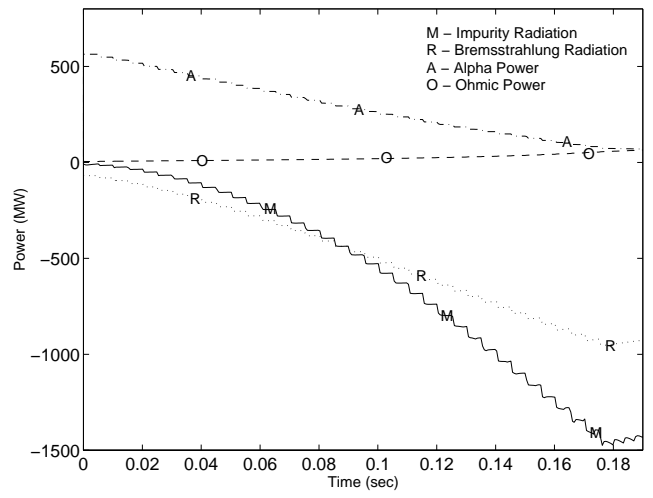
Figure 5 show the evolution of the plasma temperature during the full 2.4 s shutdown sequence. The gradual decay of the temperature during this period is a compromise between keeping the temperature high, and thus being unable to reduce the plasma current, and reducing the temperature too quickly, and thus generating large internal electric fields and hence large runaway currents. The trajectory of the plasma in the  $(I_i, q_{Edge})$  space is shown in Fig. 6, illustrating that it can be kept within the stable operating space throughout the entire sequence. The ITER PF coil currents are shown as a function of time in Fig. 7.

The plasma density increases by about a factor of eight in this sequence due to the injection of the deuterium pellets. This implies that the plasma temperature decreases by a factor of eight just due to the density increase at constant energy. This process alone would decrease the plasma temperature from 20 keV to just a few keV, and is greatest at the plasma edge where the density buildup is greatest. The remaining decrease to around 100 eV is due to the radiation cooling which tends to be very uniform, keeping the plasma pressure profile nearly self-similar as it decays. The majority of the 1 GJ of plasma energy is radiated away in about 1 s. After this time, the ohmic heating increases to about 800 MW and a balance is achieved for the next several seconds where the ohmic heating power input is radiated away by the impurity radiation at a plasma temperature





a. A close-up of the pellet trajectories



b. The associated radiative power during the first 200ms of the sequence.

Figure 4:

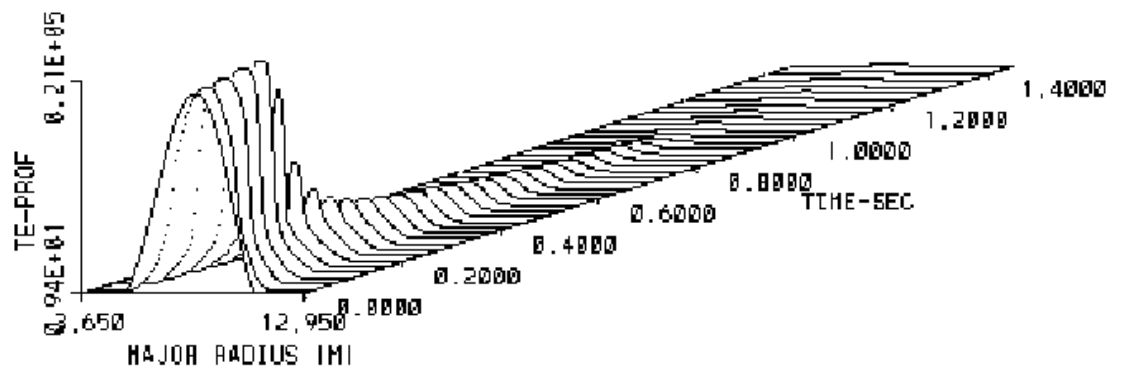


Figure 5: The plasma temperature drops to a low temperature around 100 eV during the pellet induced thermal quench with ramping down all PF coil currents. Due to the low krypton concentration on the deuterium pellets, the plasma temperature decays slowly and uniformly through the radiation. The plot shows the 3D electron temperature profile as a function of time and the major radius.

t

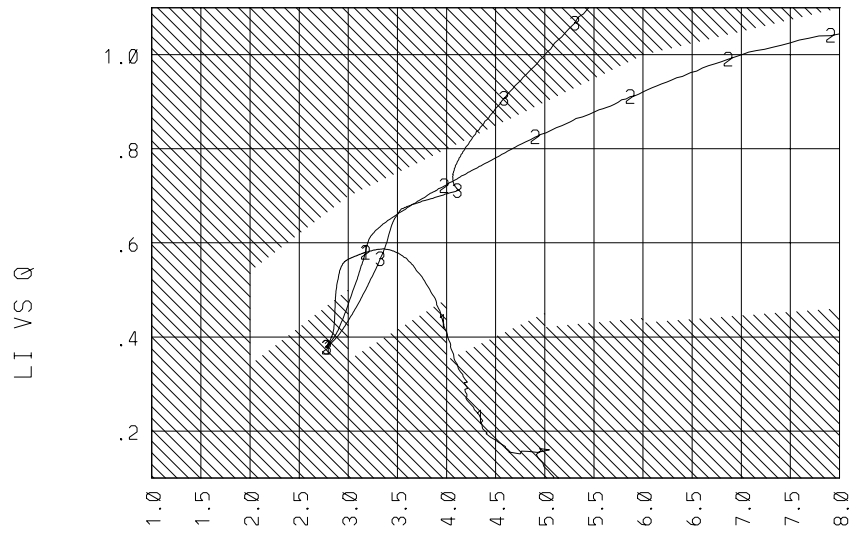


Figure 6: The trajectory of the plasma in the  $(l_i, q_{Edge})$  space for several cases: (1) - No ramp-down of PF coil currents, (2) - 4 sec ramp-down time, (3) - 2.5 sec ramp-down time. Note that detailed analysis shows the initial state to be MHD stable even though it lies in the shaded region.

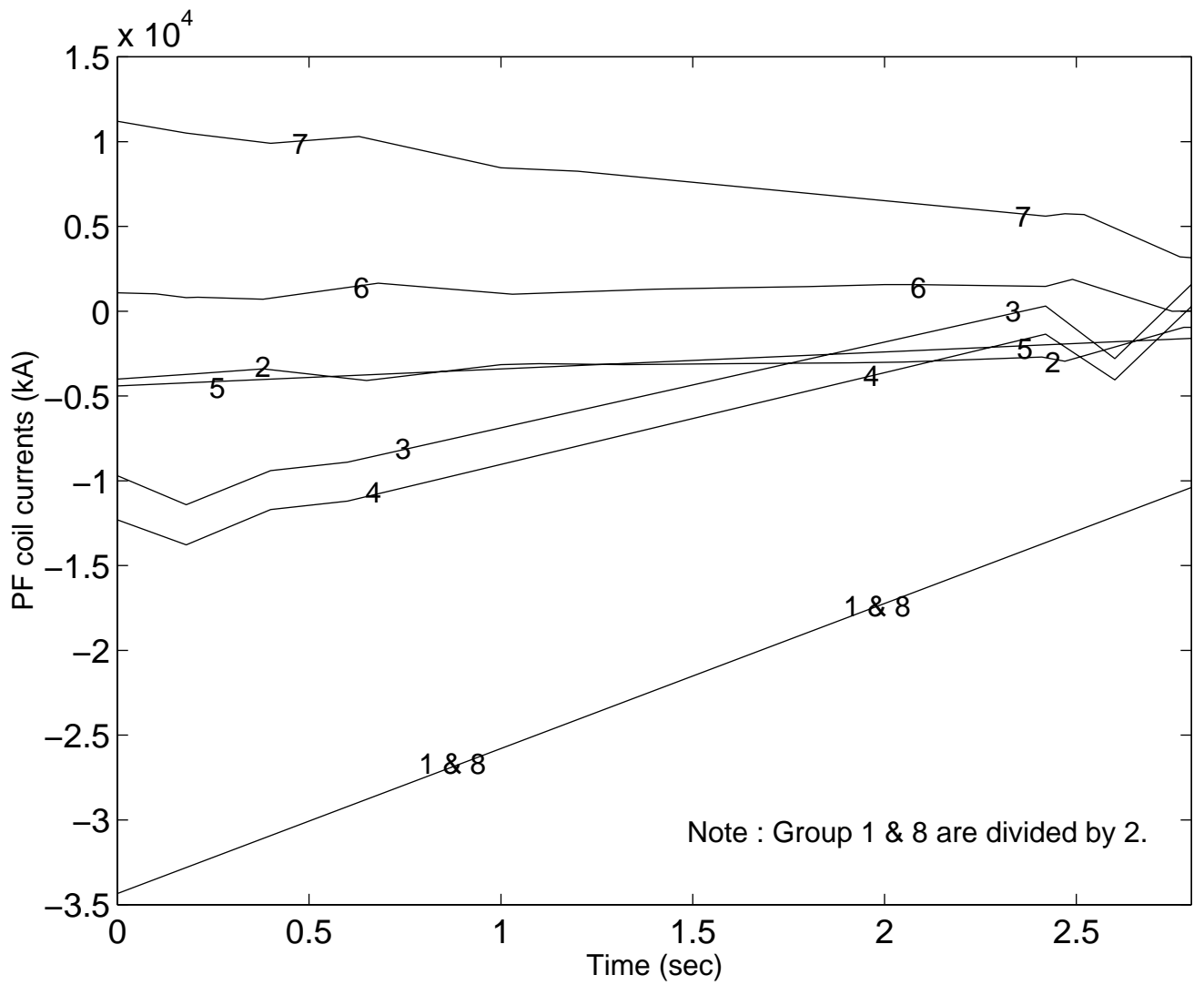


Figure 7: The ITER PF coil currents as a function of time

Group	R-position	Z-position	Feedback
1	2.448	3.024	OFF
2	5.729	9.500	ON
3	13.150	7.700	ON
4	14.965	-2.445	ON
5	13.154	-7.427	OFF
6	9.360	-9.450	ON
7	5.729	-9.500	ON
8	2.448	-3.024	OFF

Table 1: The position and the feedback system of each group coil

of a few hundred ev. This temperature is high enough to avoid substantial amounts of runaways from forming, except possibly at the edge. They are suppressed there by the negative loop voltage coming from the ramp of the PF coils.

## 4 Sensitivity to Parameters

The sequence detailed in Sec. 3 had all the desirable properties of a fast shutdown technique, but the question arises as to the sensitivity of the method to the exact details of the pellet parameters and the timings. To this end, we have carried out many variations of the simulation presented in Sec. 3 with differing numbers of pellets being injected, different Krypton concentrations, and different rampdown times for the PF coil currents.

The sensitivity of the sequence to number of pellets and Krypton concentration at fixed rampdown time are illustrated in figure 8. Shown here are the computed runaway electron currents generated (left axis), plasma current rampdown time (numbers on graph) and MHD stability indicator (symbols on graph) for a range of simulations with the number of pellets injected varying from 10 to 45, and the Krypton concentration varying from 0.005% to 0.0003%. The coil current rampdown time was fixed at  $t_{Ramp} = 4.0$  s for these calculations. The open circles indicate that the plasma  $(l_i, q_{Edge})$  trajectory remained within the stable region for the entire time, while open diamonds indicate that the trajectory crossed over into the unstable region during the current rampdown. The large polygonal region on the graph is the acceptable region. It is seen to extend to large number of pellets if the Krypton concentration is low enough, but to be limited to Krypton concentrations less than about 0.0005%. However, we find in the simulations that if the Krypton concentration falls much below 0.0003%, the radiative collapse is too slow to allow the PF coils to ramp the plasma current down in a timely manner, and a VDE may develop.

Simulations were also performed that were identical to the “standard” 4 s coil current rampdown case but that had either no ramp-down of the PF coil currents, or a faster coil current rampdown,  $t_{Ramp} = 2.5$  s. As seen in the comparison plot in Fig. 3, for the sequence without PF coil current ramp-down, the plasma current decays at about half the rate of the standard case, and over 5 MA of runaway electrons are generated due to the large electric fields that appear near the plasma edge after the pellets have been injected. To better understand this effect, we plot in Fig. 9 the ratio of the electric field

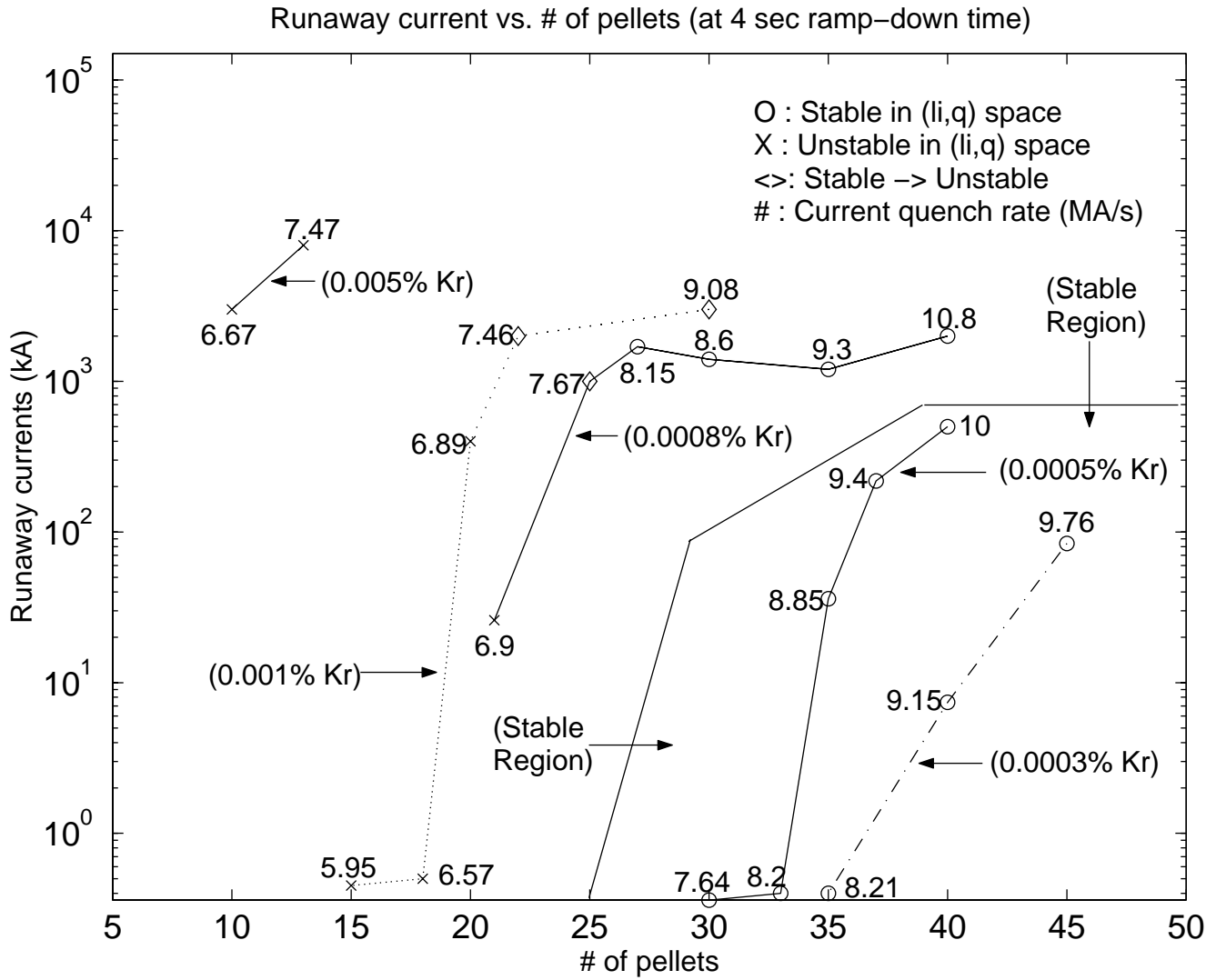


Figure 8: A range of cases with differing Kr concentrations and number of pellets shows a large stable operating region.

in the plasma to the critical electric field from Eq. 4 for 3 locations in the plasma, inner, midway, and outer, for the standard case (b) and for the no-rampdown case (a). We see that it is in the outer surfaces where  $E/E_c$  significantly exceeds 1 in the no-rampdown case, but by ramping the plasma current down, it can be kept below 1 for most of the termination period, thus effectively eliminating the generation of runaway electrons.

There is also a difficulty in the evolution of the current density in the both the no ramp-down case and the 2.5 s rampdown case. In Fig. 6 we compare the trajectories of these 2 cases with the reference case. It is seen that the no-rampdown case develops too flat of a current profile (low  $l_i$ ) and the faster 2.5 s rampdown case develops too peaked of a current profile (high  $l_i$ ), taking them into the unstable regimes in that diagram. A PF current rampdown rate of about 4 seconds appears to be essential to maintain a stable discharge during this process.

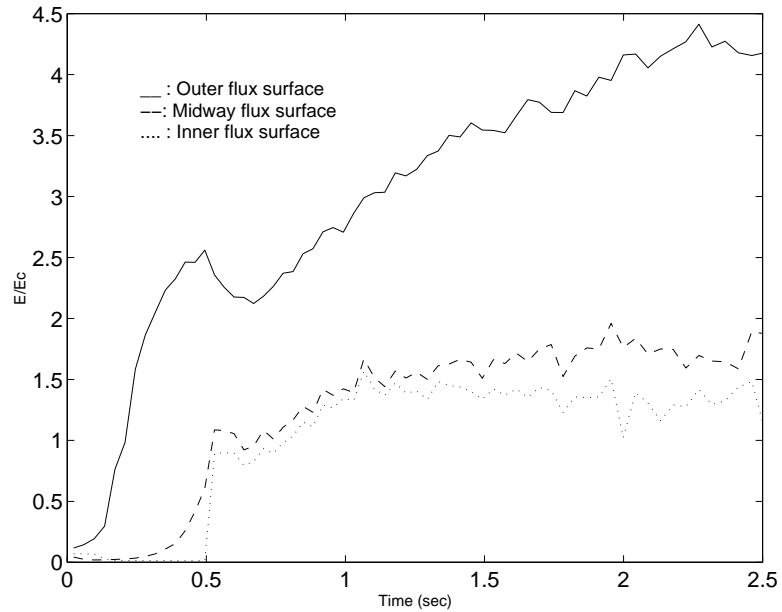
## 5 Experimental Validation

Many of the effects predicted in the simulations presented in this paper have some experimental validation. Of particular significance are the Krypton pellet shots performed in TFTR in 1997. These have been simulated with TSC using the same model presented here and provide some important validation of both the technique and the model.

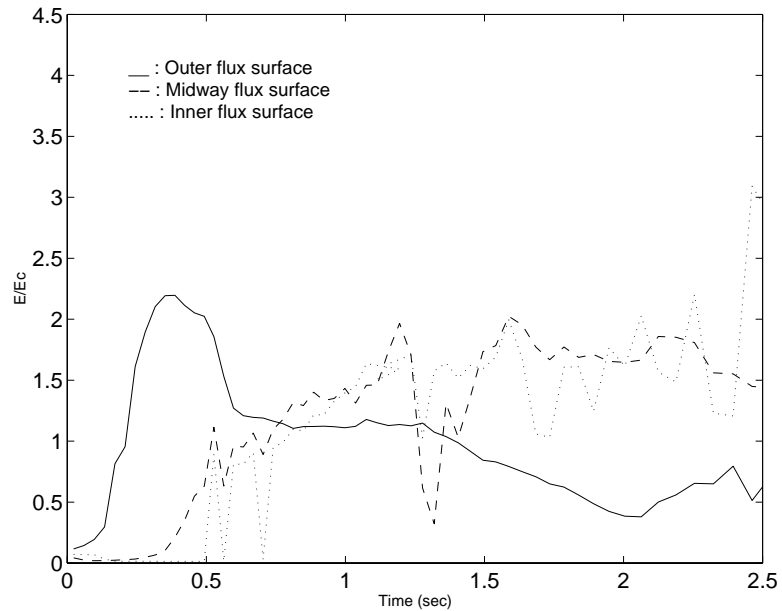
Figure 10 shows a comparison of experimental and TSC simulation results for TFTR shot 90384. This was a 1MA discharge that had 6.5 MW of neutral beam injection starting at  $t = 3.0$  sec. Two pellets were injected at times  $t = 3.502$  s and  $t = 3.504$  s. These had velocity  $v = 1200$  m/s radius  $r = 1.9$  mm, and Krypton fraction  $X = 0.06\%$ . The plasma current control system remained on until time  $t = 3.7$  s when it “tripped” and began to ramp towards zero. We simulated this shot with TSC, using the same pellet injection model described here and using the TFTR model developed previously and reported in [10]. In TSC, as in the experiment, we left the plasma current feedback control system on until  $t = 3.7$  s and then disengaged it. Four comparison traces of this shot are shown in the figure. It is seen from the diamagnetic flux and the  $\beta_p + l_i/2$  plots that the TSC simulation adequately reproduced the energy loss due to the pellet. TSC also reproduced the observed 100 ms plasma current ramp-down and verified that the discharge remained in the stable region of the  $(l_i, q_{Edge})$  space during this period. This is an initial verification of the viability of using a impurity doped pellet to cool a high temperature plasma enough so that a rapid current rampdown becomes possible. However, the runaway generation part of the model was not directly verified by these experiments since the timescales were too short for substantial avalanche production to occur.

## 6 Summary and Discussion

The fast shutdown technique being proposed here has the two critical elements: (1) injection of a sequence of impurity doped deuterium pellets, and (2) simultaneous rampdown of the currents the PF coils. The injection of a sequence of pellets with a small impurity concentration rather than a single pellet with a larger concentration facilitates penetration to the core and uniform distribution of the impurity. This allows the plasma energy to radiate away but still keep a stable pressure and current profile. The large electric fields



a. Injecting pellets only.



b. Ramp-down PF coil currents in addition to pellet injection

Figure 9: During the plasma termination, the runaway electrons and the secondary run-aways due to the avalanche effect exist when the toroidal electric field ( $E$ ) is larger than the critical electric field ( $E_c$ ). The plot shows the ratio of electric fields as a function of time.



### TSC Simulation of TFTR Krypton Pellet Shot 90384

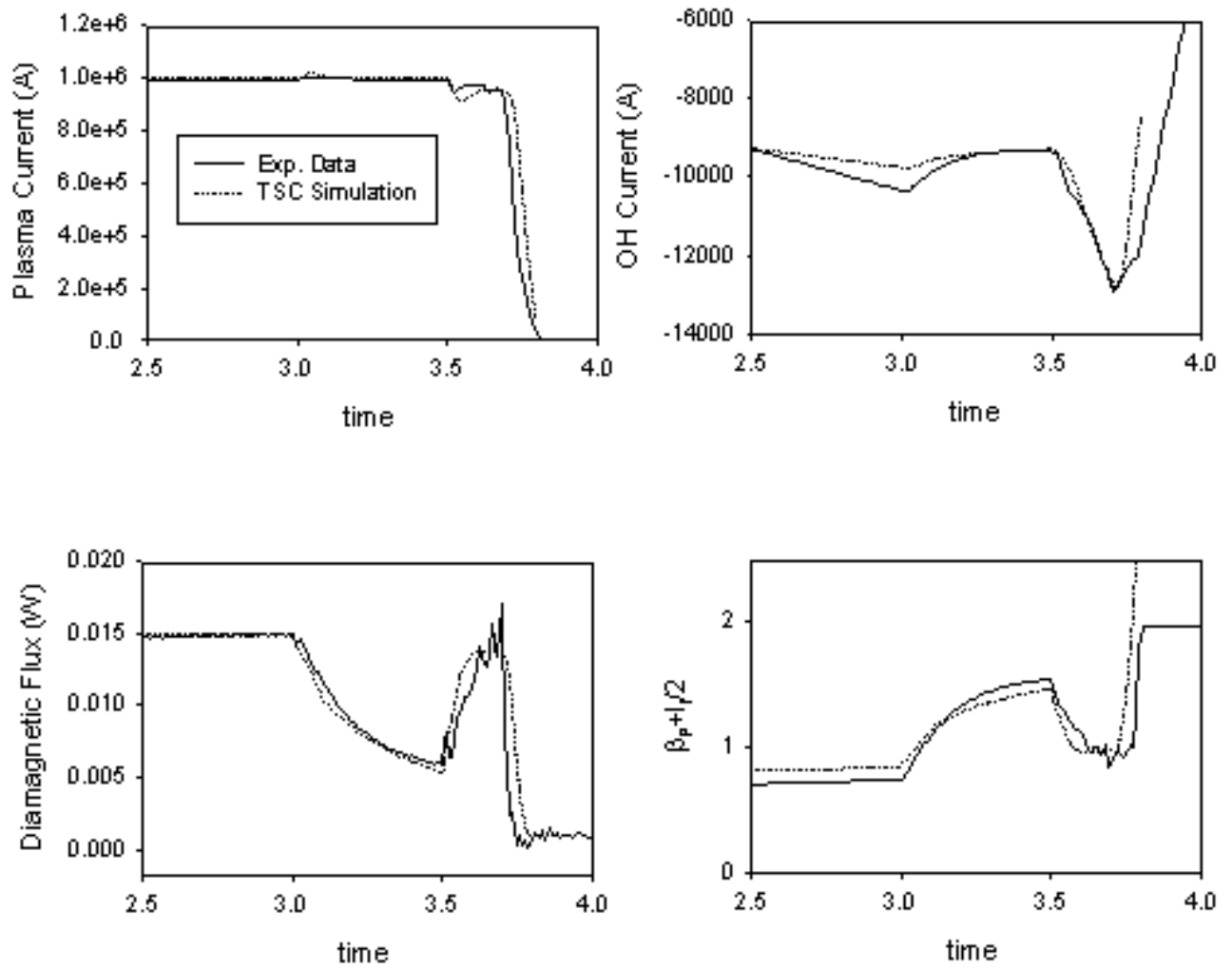


Figure 10: TFTR simulation of TFTR Krypton pellet shot 90384

that tend to be generated at the plasma edge during this process are mitigated by the negative electric fields produced by the PF system. The ramp down of the PF coils thus serves to reduce the plasma current, prevent the generation of significant numbers of runaways, and reduce the plasma elongation and thus reduce the likelihood and consequences of a VDE occurring.

We find that it is essential that the concentration of the Krypton impurity remain small, but not be zero. As the Krypton density is increased, the plasma temperature will decrease too rapidly and a substantial number of runaways will be formed. If the Krypton fraction is too small or zero, the plasma will not cool down enough to allow the PF currents to ramp the plasma current down in a timely manner, and a VDE is likely. However, detailed simulations presented here show a stable window exists in that it should be possible to avoid the generation of large numbers of runaway electrons, and that the plasma should remain stable during the entire period and avoid a VDE if the Krypton fraction is low enough but non-zero. As shown in Fig. 8, there appears to be a large stable operating window, which favors more pellets of smaller concentration. A partial experimental verification of this process has been performed on TFTR.

## **7 Acknowledgements**

We have benefited from discussions with Drs. M.N Rosenbluth, J. Wesley, S. Putvinski, P. B. Parks, D. Steiner, and with members of the ITER MHD Expert Group. This work was supported by U.S. Department of Energy Contract No. DE-AC02-76-CHO-3073.

## References

- [1] B. V. Kuteev, V. Yu. Sergeev, S. Sudo, “Emergency discharge quench or rampdown by a noble gas pellet”, *Nuclear Fusion*, **35** (1995) 1167
- [2] M. Rosenbluth, P. Parks, D. Post, S. Putvinski, N. Putvinskaya, H. A. Scott, “Runaway Electrons and Fast Plasma Shutdown”, IAEA-CN-64/FP-26, Sixteenth IAEA Fusion Energy Conference Montreal, Canada 7-11 October 1996
- [3] S. Putvinski, P. Barabaschi, N. Fujisawa, N. Putvinskaya, M. N. Rosenbluth, and J. Wesley, “Halo current, runaway electrons and disruption mitigation in ITER”, *Plasma Phys. Control. Fusion*, **39** (1997) B157
- [4] R. Yoshino, T. Kondoh, Y. Neyatani, K. Itami, Y. Kawano and N. Isei, “Fast plasma shutdown by killer pellet injection in JT-60U with reduced heat flux on the divertor plate and avoiding runaway electron generation” *Plasma Phys. Control. Fusion* **39** (1997) 313
- [5] D. G. Whyte, T. E. Evans, A. W. Hyatt, T. C. Jernigan, R. L. Lee, A. G. Kellman, P. B. Parks, R. Stockdale, and P. L. Taylor, “Rapid inward impurity transport during impurity pellet injection on the DIII-D Tokamak”, *Phys. Rev. Lett*, **81** (1998) 4392
- [6] R. D. Gill, “Generation and loss of runaway electrons following disruptions in JET”, *Nuclear Fusion*, **33** (1993) 1613
- [7] S. Putvinski, N. Fujisawa, D. Post, N. Putvinskaya, M. N. Rosenbluth, and J. Wesley, “Impurity fueling to terminate Tokamak discharges”, *Journal of Nuclear Materials*, **241-243** (1997) 316
- [8] M. N. Rosenbluth, S. V. Putvinski, P. B. Parks, “Liquid jets for fast plasma termination in tokamaks”, *Nuclear Fusion*, **37**(1997) 955
- [9] S. C. Jardin, N. Pomphrey, and J. De.ucia, “Dynamic Modeling of Transport and Positional Control of Tokamaks” *J. Comput. Phys.* **66** (1986) 481
- [10] S. C. Jardin, M. G. Bell, N. Pomphrey “TSC Simulation of Ohmic Discharges in TFTR”, *Nucl. Fusion*, **33** (1993) 317
- [11] R. O. Sayer, Y. K. Peng, S. C. Jardin, A. G. Kellman, J. C. Wesley, “TSC Plasma Halo Simulation of a DIII-D Vertical Displacement Episode”, *Nucl. Fusion*, **33** (1993) 969
- [12] L.R.Baylor, et al., *Nucl. Fusion* **32**, 2177 (1992)
- [13] G. Schmidt and S. C. Jardin, to be published, 1999
- [14] R. Jayakumar, H. H. Fleischmann, S. J. Zweben, “Collisional avalanche exponentiation of runaway electrons in electrified plasmas.”, *Phys. Lett. A* **172** (1993)
- [15] R. H. Cohen, “Runaway Electrons in an Impure Plasma,” *Physics of Fluids*, **19** (1976) 239

- [16] M. N. Rosenbluth, S. V. Putvinski, “Theory for avalanche of runaway electrons in tokamaks”, *Nuclear Fusion*, **37** (1997) 1355
- [17] H. R. Strauss and W. Park, “Magnetohydrodynamic effects on pellet injection in tokamaks”, *Physics of Plasmas*, Vol. 5, (1998) 2676
- [18] B. J. Merrill and S. C. Jardin, “Coolant Ingress Induced Disruption Calculations for ITER”, *Fusion Technology*, **19**, 1278 (1991)
- [19] R. A. Hulse, “Numerical Studies of Impurities in Fusion Plasmas”, PPPL-1917, Princeton Plasma Physics Laboratory, September (1982)
- [20] D. E. Post, et al., “Steady State Radiative Cooling Rates for Low Density, High Temperature Plasma”, *Atomic Data and Nuclear Data Tables*, **20**, (1977) 397
- [21] C. Z. Cheng, H. P. Furth, and A. H. Boozer, “MHD Stable Regime of the Tokamak”, *Plasma Physics and Controlled Fusion* **29** (1987) 351
- [22] ITER TAC-4 Physics Report, presented at 4th meeting of the ITER Technology Advisory Committee
- [23] R. Jaspers, N. J. Lopes Cardozo, F. C. Schuller, K. H. Finken, T. Grewe, G. Mank, “Disruption generated runaway electrons in TEXTOR and ITER”, *Nuclear Fusion*, **36** (1996) 367